The performance of the LHCb Pixel Hybrid Photon Detectors in a 25ns structured test–beam

Davide L. Perego, on behalf of the LHCb RICH Collaboration

***Abstract*—Particle identification plays an important role in the challenging physics programme of the LHCb experiment. Pion-kaon separation in the wide momentum range 1-100 GeV/c will be achieved by a pair of Ring Imaging Cherenkov detectors, using three radiators. Cherenkov photons in the wavelength range 200–600 nm will be detected by pixel Hybrid Photon Detectors (HPDs) developed by LHCb in collaboration with industry. The HPDs and associated electronics have been designed to operate at 40 MHz, the bunch–crossing frequency of the LHC. Final production photon detectors and the full readout chain, coupled to the LHCb data handling system, have been tested for the first time in a particle beam, operating with the nominal 25 ns bunch spacing, in September 2006. A total of 48 HPDs mounted on three RICH columns have been installed inside a customised RICH detector using N_2 and C_4F_{10} gas radiators and exposed to a 80 GeV/c pion beam at the CERN Super Proton Synchrotron. The results of the tests demonstrate that the HPD is a reliable photon detector that meets the LHCb stringent requirements on photon detection efficiency and Cherenkov angle resolution.**

LHCb-PROC-2007-036
29/10/2007

I. Introduction

THE LHCb experiment at the LHC has been optimized for high precision measurements in the beauty quark sector [1], [2]. Its main objective is to precisely determine and over–constrain the parameters of the CKM mixing matrix, and to search for further sources of CP violation and New Physics beyond the Standard Model in rare decays of B–hadrons.

Particle identification over the range 1–100 GeV/c is crucial to many LHCb analyses and it will be provided by two Ring Imaging CHerenkov (RICH) detectors which use solid silica aerogel and C_4F_{10} and CF_4 gas radiators. The RICH system uses custom–built pixel Hybrid Photon Detectors (HPDs) [3] to collect the Cherenkov photons over the wavelength range 200–600 nm. Details on the HPD can be found elsewhere [4].

The HPD has been developed and optimized in close collaboration with industry. Previous beam tests [5], [6] have successfully tested the design of individual components and demonstrated that the HPD is a reliable photon detector that meets the LHCb stringent requirements on photon detection efficiency and Cherenkov angle resolution.

To test the overall performance of the final components and exercise the complete RICH operation and data acquisition (DAQ) system, a dedicated beam test has been performed in September 2006 at the SPS facility at CERN. The time structure of the particle beam has been configured to match the operating conditions of the LHC (25 ns bunch spacing).

Manuscript created on October 2, 2007; revised November 23, 2007.

D. L. Perego is with the Istituto Nazionale di Fisica Nucleare, Sez. Milano–Bicocca, Piazza della Scienza 3, 20126 Milano Italy (tel: +39–0264482507, fax: +39–0264482463, e–mail: Davide.Perego@mib.infn.it).

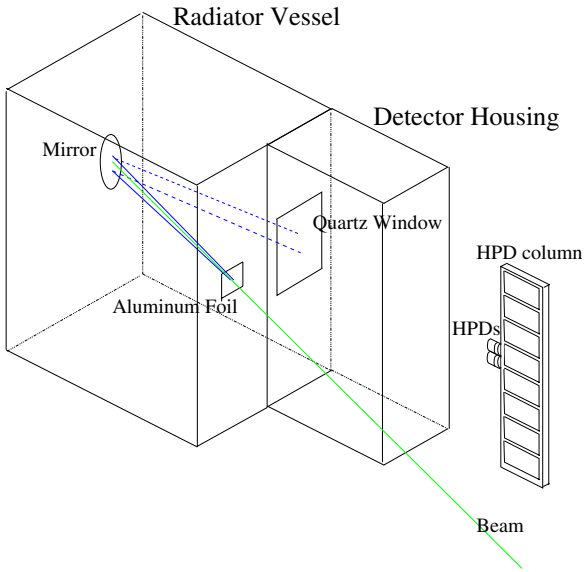

Fig. 1. Overview of the set–up used in the beam test. The green line indicates the direction of the particle beam, the blue lines represent the trajectory of (some) Cherenkov photons. To simplify the illustration, only one detector column with two HPDs is shown whereas three fully mounted columns were used during the test.

A total of 48 HPDs from the final production batch have been installed in the set–up together with the final versions of the readout electronics and DAQ system to be used for the physics data–taking with the LHCb experiment. The data quality has been monitored online with an early version of the LHCb RICH online–monitoring software. Data are analysed using the full LHCb reconstruction and analysis software framework and simulation studies are performed using the official LHCb simulation and digitization software. This test therefore provides a unique opportunity to check the RICH operations, DAQ and subsequent analysis in an environment as close to the one anticipated for the LHCb experiment as possible. This test is therefore an important milestone in the commissioning phase of the RICH system.

II. Experimental set–up

Figure 1 shows the experimental set–up of the RICH detector used during the test. The detector consists of a leak– and light–tight radiator vessel filled with either gaseous N_2 or C_4F_{10} as Cherenkov radiators. A beam consisting mainly of $\sim$80 GeV/c pions with small fractions of kaons, protons and electrons was spilled from the CERN Super Proton Synchrotron directed through the radiator vessel. Beam particles entered through a thin aluminium foil window. Cherenkov

photons created by the particles traversing the ∼1 m long radiator are reflected and focused by the tilted parabolic mirror onto the photon detectors placed outside the beam acceptance. This parabolic mirror has a focal length f of 1016 mm, a diameter of 200 mm and a reflectivity of more than 90% over the wavelength range of 225–450 nm.

The photon detector volume of the set–up is separated from the gas enclosure by a transparent quartz window and contains three fully assembled RICH columns. Each column consists of 16 HPDs with the corresponding low– and high–voltage supplies and readout electronics. The HPDs were arranged in the same hexagonally close–packed configuration as in the LHCb experiment. The detector plane is fixed at a distance of 1047 mm from the mirror centre located such that the Cherenkov rings produced by the N_2 radiator are fully contained within a single HPD. In addition, the vessel is also equipped with light–emitting diodes, useful for dedicated measurements of several HPD properties (such as dark counts, charge sharing, noise). The intensity of the LED light source was chosen such that the least illuminated HPDs were hit by 1 or 2 photons per trigger.

In order to provide the beam particle trajectory, two bare silicon pixel anodes from the HPD production were placed on either side of the RICH in the beam and equipped with readout electronics. The upstream tracking station was placed at a short distance in front of the aluminium entrance window, while the downstream station just behind the parabolic mirror at the end of the gas volume. The two pixel chips were both positioned with their sensitive side facing the radiator volume in order to limit the effect of the multiple scattering of the beam through the pixel chips. The chips were also tilted backwards away from the radiator volume so that the beam would not pass through the Level–0 electronics placed behind them. The pixel chips were connected to the same Level–0 data acquisition electronics as used for the HPDs used to detect the Cherenkov light. Consequently the tracking devices could be triggered and read out in the same way as the HPDs.

The set–up was completed by the installation of a pair of plastic scintillators placed along the flight path of the beam particles. A coincident signal from both scintillators was used to trigger the event.

III. Photoelectron Yields

The efficiency of a RICH detector can be evaluated by counting the number of photons detected on Cherenkov rings produced in the radiator. The ultimate aim of the photoelectron yield studies is the determination of a model for photoelectron production and detection that can be checked on the beam test data and used to calculate the expected number of detected photoelectrons per charged particle in the final experiment.

The gas vessel was filled with two different Cherenkov radiators during the test, dry N_2 and C_4F_{10}. In case of N_2, thanks to its low refractive index the Cherenkov ring is fully contained on a single HPD. Data were taken on three different HPDs. The use of C_4F_{10} has a twofold advantage: this is the gas to be used in RICH1 detector, so that results from the beam test can be easily translated to the final detector; secondly, its refractive index (and therefore the Cherenkov angle θ_C) is big enough that the ring in the photon detection plane covers up to four HPDs, allowing timing and performance studies and cross–checks of the electronics on all the columns at the same time. Figure 2 shows examples of Cherenkov rings from N_2 and C_4F_{10} runs.

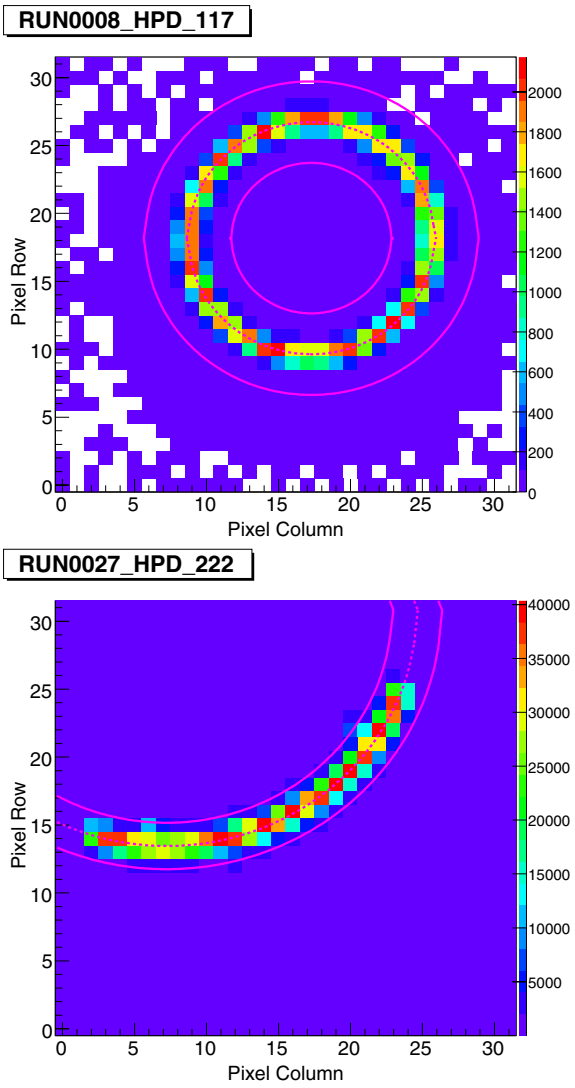

Fig. 2. The hit pixels in events integrated over an entire run in the same radiator for N_2 (*top*) and C_4F_{10} (*bottom*). Superimposed on the hit distributions are the average ring and the road for each run.

A. Event Selection

An unambiguous definition of the ring region is needed in order to proceed with photoelectron counting. Hits are then considered to originate from a Cherenkov photon if they lie within a well–defined region around the average Cherenkov ring. The number of hits in this "road" per event is then taken as the figure of merit for the Cherenkov photoelectron yield and detection efficiency. To disantangle as much as possible from ion feedback and background hits induced by radiation timed with the beam or similar unpredictable effects, events are selected if at least four hits are within the road and rejected

if more than three hits are recorded outside the road. The width of the road around the average Cherenkov ring is fixed to $\Delta R = 3$ pixels in N_2 runs, while in C_4F_{10} studies, ΔR has been assumed to be one sigma (σ_R) of the ring radius distributions, with an average value of about 1.7 pixels.

B. Photoelectron Yield: the model

The photoelectron yield is extracted by a constrained fit to the distribution, $N(n)$, of hit pixels on an event–by–event basis. The model takes into account several contributions:

- pixel–to–pixel charge sharing fraction, s, where one photoelectron produces hits in two neighbouring pixels;
- double hits fraction, d, where hits are lost due to two photoelectrons striking a single silicon pixel but only one hit being recorded because of the the binary readout of the pixel chip;
- multiple particle occupancy in the beam;
- the beam composition, a mixture of charged particles, approximately 80% π, 10% e, 7% K and 3% p above the Cherenkov threshold.

Assuming saturated electrons to be indistinguishable from the pion fraction of the beam, the histogram of hit pixels per event $N(n)$ is described by:

$$N(n) = \sum_{i=\pi,K,p} N_{1,i} \cdot P(n;\mu_i,s,d) + N_2 \cdot P(n;2\mu,s,d) + \dots \tag{1}$$

where:

$$P(n;\mu,s,d) = \sum_{i=0}^{n} \sum_{j=0}^{\infty} P(n-i+j;\mu) \times P(i;(n-i)s) \times P(j;(n-i+j)(n-i+j-1)d) \tag{2}$$

and $P(a;b)$ is the Poisson probability of getting a given a mean value b. The relation in (1) is a sum over all the possible particle types with weights $N_{1,i}$; a two–particle and a possible three–particle terms with weights N_2 and N_3 respectively have been considered. In the multiple particle case, only pions have been assumed.

The $P(n;\mu_i,s,d)$ in (2) are Poisson–like probabilities that are the underlying Poisson distribution for the number of hits on a ring that is corrected for combinations where hits are gained due to charge sharing or lost due to the binary readout (double hits). The charge sharing fraction has been fixed for each HPD to the corresponding value measured in dedicated LED and dark count runs. The typical value of the charge sharing fraction is $\sim$3%.

The fit has been performed in the limited range between 5 and 30 hits for all runs. In case of C_4F_{10} the absolute value of μ depends on the fraction of the ring overlapping with the photocathode of the HPD under study. This fraction has been calculated from the geometric distribution of the hits on the anode, by plotting the occupancy as a function of the angle ϕ with respect to the fitted centre of the ring. The ratio $\mu/\Delta\phi$ is then used as the figure of merit for the photoelectron yield. Figure 3 shows a typical distribution of the number of hits in the road and superimposed is the resulting fit function.

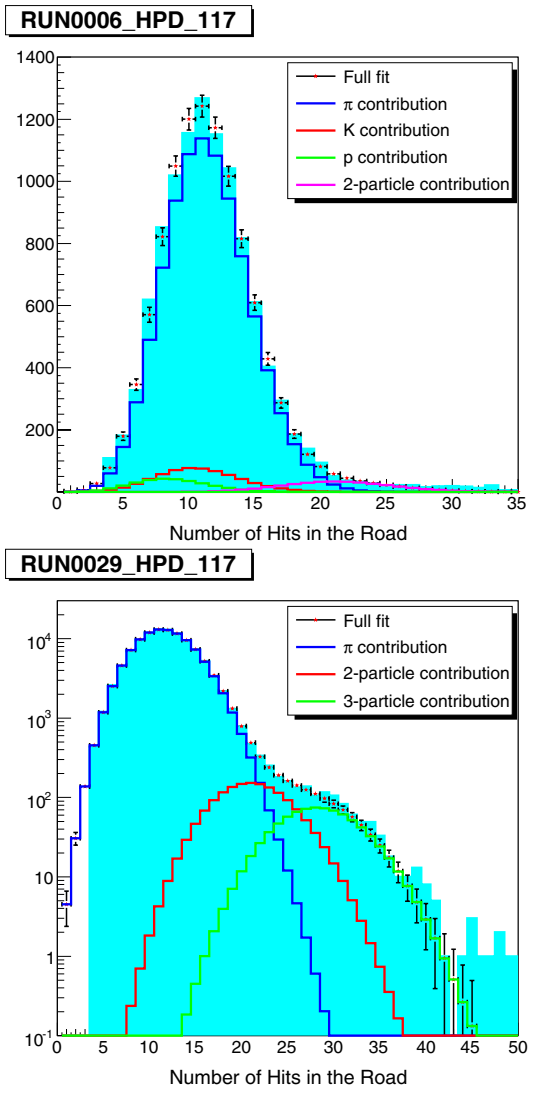

Fig. 3. Distribution of the hits in the road for the same HPD 117, in N_2 (*top*) and C_4F_{10} (*bottom*) runs. Data (full cyan histogram) and fitting functions (colour histograms) are shown.

C. Photoelectron yield analysis in N_2

The number of events with two or more particles is reduced by requiring that there is only one cluster of hits making a track in each of the tracking stations. This selects approximately 40% of events. Rings are then fitted to the N_2 events on an event–by–event basis (as shown in Figure 4) and the average ring centre and radius used to define the valid ring region ($\Delta R = 3$ pixels about this average ring position). This removes events with no Cherenkov ring or large clusters of hits on the anode that come from charge settling effects and selects 87% of the events passing the tracker cut.

The photoelectron yield μ is extracted from (1); one– and two–particle contributions in the beam and the double hit fraction are also found as free parameters in the fit. An example distribution of hit pixels with its corresponding fit can be seen in Figure 3. The χ^2/NDF found in the shown run is 31.52/23, so the model accurately reproduces the distribution seen in the data. A summary of the yields for each of the three

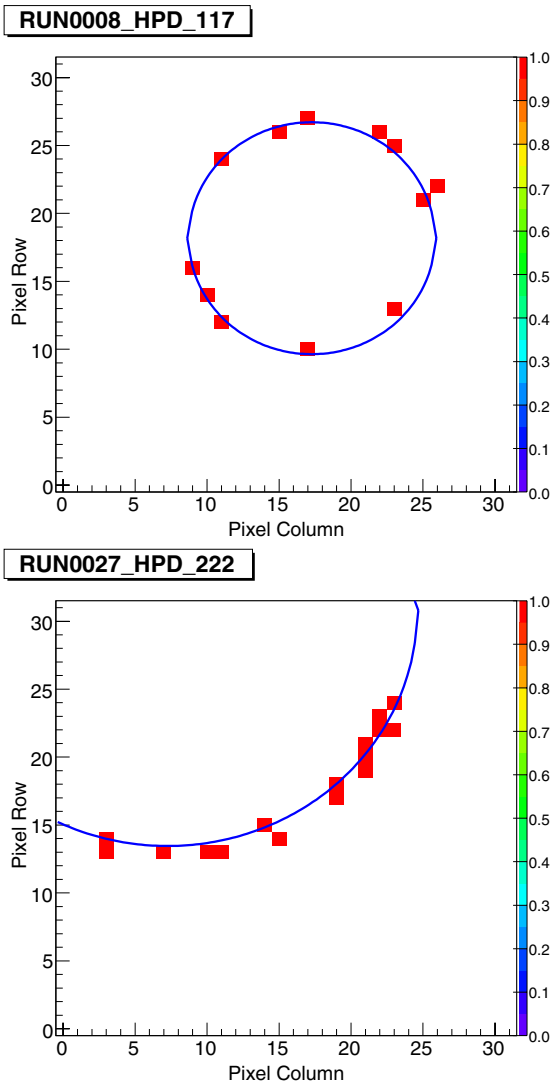

Fig. 4. The hit pixels in a typical single event in N_2 (*top*) and C_4F_{10} (*bottom*) runs. The best fit rings are superimposed.

TABLE I
MEASURED AND EXPECTED PHOTOELECTRON YIELDS FOR N_2 DATA.

HPD	Measured	Expected
117	12.32±0.12	12.20±0.62
264	13.14±0.13	14.09±0.70
265	12.56±0.12	12.81±0.65

photon detectors involved in N_2 runs is given in Table I.

The expected number of detected photoelectrons from a saturated track (β = 1) passing through a Cherenkov length L is given by:

$$N = \left(\frac{\alpha}{\hbar c}\right) L \varepsilon_A \eta \int QRT \left(1 - \frac{1}{n(E)^2\beta^2}\right) \mathrm{d}E \qquad (3)$$

where the first factor is a constant with value 370 $\mathrm{eV}^{-1}\mathrm{cm}^{-1}$, ε_A is the coverage of the photon detector active area and η is the HPD single photoelectron detection efficiency following the conversion by the photocathode. The energy–dependent terms in the integral are the HPD quantum efficiency Q, the mirror reflectivity R, the transmission T of the quartz window that separates the radiator and HPD volume and $n(E)$ the refractive index of the N_2 gas. Results are given in Table I, where the quantum efficiencies measured by the manufacturer have been used.

The largest contribution to the error on the expected yield comes from an assumed 5% error on the product of QRT. The error in Table I also includes a small contribution from pressure and temperature variations during data taking.

Systematic uncertainties that appear with the measured yield in Table I have been determined by introducing a series of Gaussian penalty terms to the fit so that the function minimised is now given by:

$$\chi^2_{fit} + \underbrace{\left(\frac{s-\bar{s}}{\sigma_s}\right)^2}_{charge\ sharing} + \underbrace{\left(\frac{d-\bar{d}}{\sigma_d}\right)^2}_{double\ hits} + \ldots \qquad (4)$$

and allow the previously fixed parameters (s, d, ...) to vary accordingly:

- the charge sharing fraction s is typically ∼3%;
- the probability to lose a hit as a double hit depends on the number of hits in the ring. In the fit the probability per hit is assumed to be linear with the event size, $(n-1)\times d$, where $d = (5 \pm 1) \times 10^{-3}$. This quantity is estimated both from a toy model and a "fake–event" method and these give comparable results. In the fake event method hits are selected at random from multiple different events to build a new event that contains only one hit from any one contributing event.
- the fraction of kaons and protons in the fit are taken to be 7 ± 2 and 3 ± 2 respectively.

From the N_2 photoelectron yield analysis the conclusion is that measured values are in good agreement with the analytic expected ones.

D. Photoelectron yield analysis in C_4F_{10}

A similar approach has been used to analyze C_4F_{10} data. Firstly the road region is defined as in the following. For each event, the fit results are the coordinates of the centre of the circle and its radius. The average values of these parameters, x_C, y_C and R, together with their standard deviations are computed for all the events in the run whose fit resulted in a $\chi^2/\mathrm{NDF} < 4$. A road is defined as the ring–like region enclosed by two concentric circles. The coordinates of the common centre of the circles are x_C and y_C, and the radii are $R \pm \sigma_R$. Figure 3 shows, for a typical C_4F_{10} run, the hit distribution on the anode and, superimposed, the road. A single event display is shown in Figure 4.

A hit on the pixel chip is considered as a genuine Cherenkov photon if it lies within the road. Events are selected if there are at least four hits within the road and no more than three recorded outside. In this way, 8% of the events are rejected on average.

The C_4F_{10} analysis assumes only one–particle species (saturated pion). Two– and three–particle terms have been added to the fit function; however, the multiple particle fraction is only ∼2% of the total.

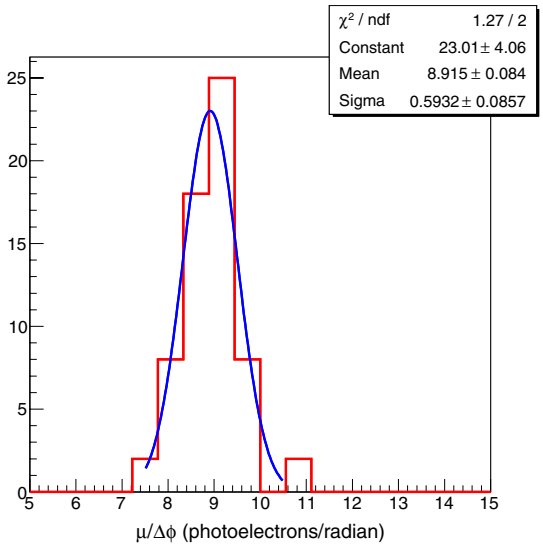

Fig. 5. Distribution of the $\mu/\Delta\phi$ values determined from C_4F_{10} data. The histogram has been fitted to a Gaussian, giving a mean value of 8.9±0.1 photoelectrons per radian.

For all the runs taken at the optimal timing setting the photolectron yield per radian $\mu/\Delta\phi$ has been calculated. To check the reproducibility of the results, the comparison of the photoelectron yield for the same HPD in different runs has been performed. The results are stable to within 5%. A possible explanation for the run to run deviations lies in a slight non–uniformity of the photocathode in terms of its quantum efficiency, since in different runs different regions of the HPDs are illuminated by Cherenkov photons. A summary of the $\mu/\Delta\phi$ results is shown in Figure 5. The average photoelectron yield is 8.9±0.1 per radian, with 10% spread from HPD to HPD. This is consistent with the different quantum efficiencies of the photon detectors measured during the quality assessment phase. Systematic uncertainties contribute at the 5% level.

A comparison with expected yields from full Monte–Carlo simulation has been done, finding good agreement.

IV. Cherenkov angle resolutions

The Cherenkov angle resolution studies started recently. This kind of analysis strongly depends on the alignment of the many parts of the detector (such as HPDs, mirror, tracking stations) and on the good knowledge of the Cherenkov gas purity. Encouraging preliminary results have been found using the ray tracing procedure.

For both N_2 and C_4F_{10} data, a single photon resolution $\sigma(\theta_C) \sim 1.6$ mrad has been found, in agreement with expectations. These excellent resolutions have been reached due to an iterative alignment procedure, but the work is still ongoing to better understand the various contributions to the resolution. A more precise calibration of the gas compositions is mandatory. Typical distributions of the Cherenkov angle θ_C for the radiators are reported in Figure 6.

V. Conclusions

The September 2006 beam test has been a very important milestone in the commissioning of the two RICH detectors

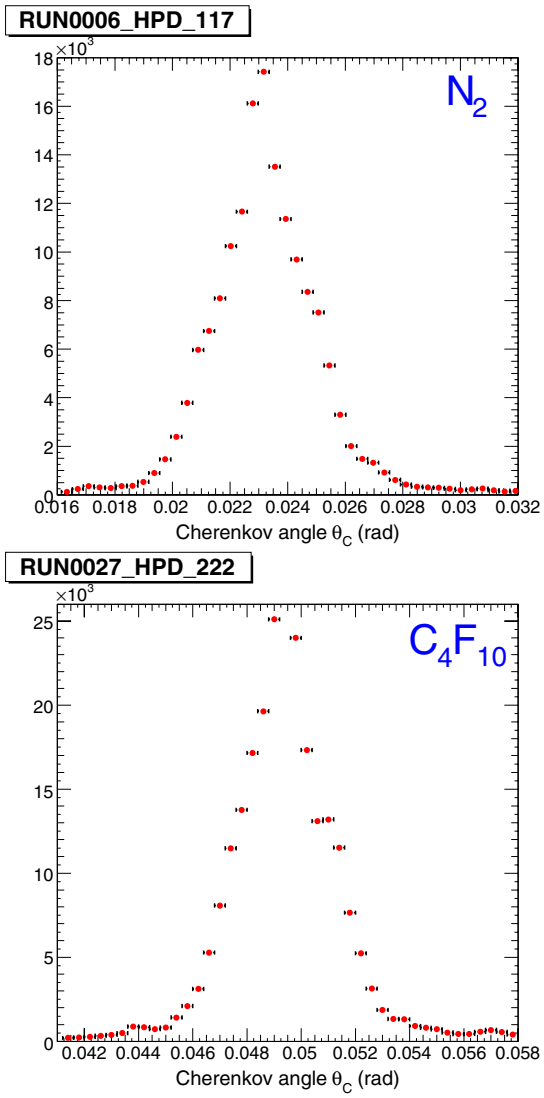

Fig. 6. Distributions of the Cherenkov angle θ_C in two typical runs with N_2 (*top*) and C_4F_{10} (*bottom*) data.

of the LHCb experiment. A set of 48 HPDs from the final production has been successfully tested together with the final versions of the readout electronics, DAQ system and software frameworks (online monitoring, reconstruction, simulation and analysis). The encouraging preliminary results demonstrate that the photon detectors to be used in the LHCb RICH detectors meet the stringent requirements in terms of photoelectron yield, efficiency and Cherenkov angle resolution.

References

[1] The LHCb Coll., LHCb Technical Proposal, CERN/LHCC/98–4 (1998).
[2] The LHCb Coll., LHCb Reoptimized Detector Design and Performance TDR, CERN/LHCC/2003–030 (2003).
[3] M. Moritz et al., IEEE Trans. Nucl. Sc. Vol. 51 No. 3 (2004), 1060.
[4] T. Blake, These proceedings.
[5] G. Aglieri–Rinella et al., Test Beam Results from a RICH Detector prototype using Aerogel radiator and pixel Hybrid Photon Detectors, CERN–LHCb–2006–006.
[6] M. Adinolfi et al., Nucl. Instr. and Meth. A 574 (2007) 39.